Quadratic electronic response of a two-dimensional electron gas

A. Bergara[1], J.M. Pitarke[1], and P. M. Echenique[2]

[1]*Materia Kondentsatuaren Fisika Saila, Zientzi Fakultatea, Euskal Herriko Unibertsitatea, 644 Posta Kutxatila, 48080 Bilbo, Basque Country, Spain*

[2]*Materialen Fisika Saila, Kimika Fakultatea, Euskal Herriko Unibertsitatea, 1072 Posta Kutxatila, 20080 Donostia, Basque Country, Spain*

(February 1, 2008)

Abstract

The electronic response of a two-dimensional (2D) electron system represents a key quantity in discussing one-electron properties of electrons in semiconductor heterojunctions, on the surface of liquid helium and in copper-oxide planes of high-temperature superconductors. We here report an evaluation of the wave-vector and frequency dependent dynamical quadratic density-response function of a 2D electron gas (2DEG), within a self-consistent field approximation. We use this result to find the Z_1^3 correction to the stopping power of a 2DEG for charged particles moving at a fixed distance from the plane of the 2D sheet, Z_1 being the projectile charge. We reproduce, in the high-density limit, previous full nonlinear calculations of the stopping power of a 2DEG for slow antiprotons, and we go further to calculate the Z_1^3 correction to the stopping power of a 2DEG for a wide range of projectile velocities. Our results indicate that linear response calculations are, for all projectile velocities, less reliable in two dimensions than in three dimensions.

I. INTRODUCTION

Since the pioneering work of Bohm and Pines[1], the conduction electrons in a metal have been described as a three-dimensional (3D) gas of electrons in a neutralizing uniform positive charge. The dynamical linear density-response function of a 3D electron gas (3DEG) was evaluated by Lindhard[2] in the so-called random-phase approximation (RPA), in which each electron is assumed to move in the external field plus the induced field of all electrons. The wave-vector and frequency dependent dynamical quadratic density-response function of a 3DEG has also been evaluated[3], by going beyond linear response theory. The knowledge of this quantity has been proved to be of great importance in discussing the properties of electrons in a variety of 3D systems[4], and, in particular, in explaining the experimentally observed difference between the electronic energy losses of protons and antiprotons moving through a solid[5,6].

The suggested existence of two-dimensional electron layers in metal-insulator-semiconductor structures and on the surface of liquid helium led several years ago to a great activity in the study of a two-dimensional electron gas[7], where the electrons are confined to a plane and neutralized by an inert uniform rigid positive plane background. The 2D electron system has also been considered in discussing the physics of new-class materials such as copper-oxide planes of high-temperature superconductors[8]. It has been found that electrons confined to a 2D layer show sometimes interesting properties not shared by a 3D electron system. For instance, for a 2D metal the plasma frequency goes to zero in the long-wavelength limit, in contrast to the 3D situation[9]. Stern[10] evaluated the dynamical linear density-response function of a 2DEG in the RPA, and calculated the plasmon dispersion and the asymptotic screened Coulomb potential. Also, much effort has gone into studying the ground state energy[11] and the excitation spectrum of a 2DEG[12]. The stopping power for a fast particle moving parallel to a 2DEG was first evaluated in the RPA, within linear response theory, by Horing *et al*[13], and the effect on this quantity of finite temperature[14], local field corrections[15] and recoil[16] has also been considered. Nonlinear calculations of the

stopping power for slow protons and antiprotons have been performed only very recently[17,18] on the basis of a scattering theory approach, the scattering cross sections being calculated for a statically screened potential.

In this paper we present results for the dynamical quadratic electronic density-response of a 2DEG to longitudinal external fields of arbitrary wave-vector and frequency, which we evaluate on the same level of approximation as the RPA linear density-response function of Stern[10]. In order to illustrate the usefulness of the knowledge of this quantity, we consider, as an example, the stopping power of a 2DEG, and we use the quadratic density-response function to evaluate the Z_1^3 nonlinear correction to the stopping power of a 2DEG for particles of charge $Z_1 e$ moving at a fixed distance from the 2D plasma.

II. DYNAMICAL ELECTRONIC RESPONSE

We consider a uniform electron system of density n_0 at zero temperature. Linear and quadratic density-response functions of this system, $\chi(x,x')$ and $Y(x,x',x'')$, with $x=(\mathbf{r},t)$, may be introduced in connection with the response to the presence of a time-varying external influence, after an expansion of the induced electron density in powers of the external potential $V(x)$. According to time-dependent perturbation theory, the induced electron density is given, up to second order in $V(x)$, by (we use atomic units throughout, i.e., $e^2=\hbar=m_e=1$)

$$n^{ind}(x)=\int \mathrm{d}x'\chi(x,x')V(x')+\int \mathrm{d}x'\int \mathrm{d}x''Y(x,x',x'')V(x')V(x''), \tag{2.1}$$

where

$$\chi(x,x')=-\mathrm{i}\,\Theta(t-t')<\Psi_0|\left[\tilde{\rho}_H(x),\tilde{\rho}_H(x')\right]|\Psi_0> \tag{2.2}$$

and

$$\begin{aligned} Y(x,x',x'')=&\Theta(t-t')\Theta(t'-t'')<\Psi_0|\left[\left[\tilde{\rho}_H(x),\tilde{\rho}_H(x')\right],\tilde{\rho}_H(x'')\right]|\Psi_0>/2\\ &+\Theta(t-t'')\Theta(t''-t')<\Psi_0|\left[\left[\tilde{\rho}_H(x),\tilde{\rho}_H(x'')\right],\tilde{\rho}_H(x')\right]|\Psi_0>/2. \end{aligned} \tag{2.3}$$

Here $|\Psi_0>$ denotes the normalized ground state, $\tilde{\rho}_H$ is the density fluctuation operator $\tilde{\rho}_H = \hat{\rho}_H - n_0$, where $\hat{\rho}_H$ is the exact Heisenberg density operator in the unperturbed system, and $\Theta(x)$ is the Heaviside step function accounting for causality.

In a self-consistent field or random-phase approximation (RPA), it is assumed that the electron density induced by an external potential can be replaced by the electron density induced in a non-interacting electron gas by the sum of the external potential, $V(x)$, and the potential created by the induced electron density itself, $V^{ind}(x)$. Hence, in this approximation:

$$\begin{aligned} n^{ind}(x) = &\int \mathrm{d}x' \chi^0(x,x') \left[V(x') + V^{ind}(x')\right] \\ &+ \int \mathrm{d}x' \int \mathrm{d}x'' Y^0(x,x',x'') \left[V(x') + V^{ind}(x')\right] \left[V(x'') + V^{ind}(x'')\right]. \end{aligned} \tag{2.4}$$

Here $\chi^0(x,x')$ and $Y^0(x,x',x'')$ are 'free-particle' linear and quadratic density-response functions, and

$$V^{ind}(x) = \int \mathrm{d}x' v(x,x') n^{ind}(x'), \tag{2.5}$$

where $v(x,x')$ represents the instantaneous Coulomb interaction. Introducing Eq. (2.5) into Eq. (2.4) and keeping in Eq. (2.4) only terms up to second order in $V(x)$, one finds the following integral equations for RPA linear and quadratic density-response functions:

$$\chi(x_1,x_2) = \chi^0(x_1,x_2) + \int \mathrm{d}x_1' \int \mathrm{d}x_2' \chi^0(x_1,x_1') v(x_1',x_2') \chi(x_2',x_2) \tag{2.6}$$

and

$$\begin{aligned} Y(x_1,x_2,x_3) = &\int \mathrm{d}x_2' \int \mathrm{d}x_3' Y^0(x_1,x_2',x_3') K(x_2',x_2) K(x_3',x_3) \\ &+ \int \mathrm{d}x_1' \int \mathrm{d}x_1'' \chi^0(x_1,x_1') v(x_1',x_1'') Y(x_1'',x_2,x_3), \end{aligned} \tag{2.7}$$

where $K(x,x')$ is the so-called inverse dielectric function:

$$K(x,x') = \delta(x-x') + \int \mathrm{d}x'' v(x,x'') \chi(x'',x'). \tag{2.8}$$

The integral equations (2.6) and (2.7) have, within many-body perturbation theory, the simple diagrammatic interpretation shown in Fig. 1, where empty and full bubbles

represent non-interacting and interacting linear density-response functions, $\chi^0(x_1, x_2)$ and $\chi(x_1, x_2)$, respectively. Similarly, empty and full triangles represent non-interacting and interacting quadratic density-response functions, $Y^0(x_1, x_2, x_3)$ and $Y(x_1, x_2, x_3)$, respectively, and dashed lines represent the Coulomb interaction, $v(x, x')$. Thus, RPA linear and quadratic density-response functions are represented diagrammatically by summing over the infinite set of diagrams containing one (see Fig. 1a) and three (see Fig. 1b) strings of empty bubbles, respectively.

In the case of a homogeneous 2DEG, the electrons are free to move in two spatial dimensions, having their motion constrained in the third dimension. Thus, assuming time invariance, we define the Fourier transforms

$$\chi_q = \int \mathrm{d}^2\mathbf{r}_1 \int \mathrm{d}t_1 \mathrm{e}^{-\mathrm{i}[\mathbf{q}\cdot(\mathbf{r}_1-\mathbf{r}_2)-\omega(t_1-t_2)]}\chi(\mathbf{r}_1, t_1; \mathbf{r}_2, t_2) \tag{2.9}$$

and

$$Y_{q_1,q_2} = \int \mathrm{d}^2\mathbf{r}_1 \int \mathrm{d}t_1 \int \mathrm{d}^2\mathbf{r}_2 \int \mathrm{d}t_2\, \mathrm{e}^{-\mathrm{i}[\mathbf{q}_1\cdot(\mathbf{r}_1-\mathbf{r}_2)-\omega_1(t_1-t_2)]}\mathrm{e}^{-\mathrm{i}[(\mathbf{q}_1+\mathbf{q}_2)\cdot(\mathbf{r}_2-\mathbf{r}_3)-(\omega_1+\omega_2)(t_2-t_3)]} \times Y(\mathbf{r}_1, t_1; \mathbf{r}_2, t_2; \mathbf{r}_3, t_3), \tag{2.10}$$

where $\mathbf{r}_1$, $\mathbf{r}_2$ and $\mathbf{r}_3$ represent two-dimensional position-vectors in the 2D plane, and q is the trimomentum $q = (\mathbf{q}, q^0)$. Hence, within the RPA we find:

$$\chi_q = \chi_q^0 + \chi_q^0 v_q \chi_q \tag{2.11}$$

and

$$Y_{q,-q_1} = Y^0_{q,-q_1} K_{q_1} K_{q-q_1} + \chi_q^0 v_q Y_{q,-q_1}, \tag{2.12}$$

where

$$K_q = 1 + v_q \chi_q \tag{2.13}$$

and $v_q = 2\pi/|\mathbf{q}|$.

For a non-interacting Fermi gas, the ground state is obtained by filling all the plane wave states inside the Fermi sphere of radius $q_F = \sqrt{2}/r_s$, r_s being the average interelectronic

distance ($n_0^{-1} = \pi r_s^2$). As in the case of a 3DEG[19], we find non-interacting linear and quadratic density-response functions to be[20]

$$\chi_q^0 = 2\int \frac{\mathrm{d}^2\mathbf{k}}{(2\pi)^2}\left[\frac{n_{\mathbf{k}}(1-n_{\mathbf{k}+\mathbf{q}})}{q^0-(\omega_{\mathbf{k}+\mathbf{q}}-\omega_{\mathbf{k}})+\mathrm{i}\eta}+\frac{(1-n_{\mathbf{k}})n_{\mathbf{k}+\mathbf{q}}}{-q^0-(\omega_{\mathbf{k}}-\omega_{\mathbf{k}+\mathbf{q}})-\mathrm{i}\eta}\right] \tag{2.14}$$

and

$$\begin{aligned} Y_{q,-q_1}^0 = -\int \frac{\mathrm{d}^2\mathbf{k}}{(2\pi)^2}[\quad & \frac{n_{\mathbf{k}}(1-n_{\mathbf{k}+\mathbf{q}})(1-n_{\mathbf{k}+\mathbf{q}_1})}{(q^0+\omega_{\mathbf{k}}-\omega_{\mathbf{k}+\mathbf{q}}+\mathrm{i}\eta)(q_1^0+\omega_{\mathbf{k}}-\omega_{\mathbf{k}+\mathbf{q}_1}+\mathrm{i}\eta)} \\ & - \frac{(1-n_{\mathbf{k}})n_{\mathbf{k}+\mathbf{q}}n_{\mathbf{k}+\mathbf{q}_1}}{(q^0+\omega_{\mathbf{k}}-\omega_{\mathbf{k}+\mathbf{q}}+\mathrm{i}\eta)(q_1^0+\omega_{\mathbf{k}}-\omega_{\mathbf{k}+\mathbf{q}_1}+\mathrm{i}\eta)} \\ & + \frac{n_{\mathbf{k}+\mathbf{q}}(1-n_{\mathbf{k}})(1-n_{\mathbf{k}+\mathbf{q}_1})}{(-q^0+\omega_{\mathbf{k}+\mathbf{q}}-\omega_{\mathbf{k}}-\mathrm{i}\eta)(-q^0+q_1^0+\omega_{\mathbf{k}+\mathbf{q}}-\omega_{\mathbf{k}+\mathbf{q}_1}-\mathrm{i}\eta)} \\ & - \frac{(1-n_{\mathbf{k}+\mathbf{q}})n_{\mathbf{k}}n_{\mathbf{k}+\mathbf{q}_1}}{(-q^0+\omega_{\mathbf{k}+\mathbf{q}}-\omega_{\mathbf{k}}-\mathrm{i}\eta)(-q^0+q_1^0+\omega_{\mathbf{k}+\mathbf{q}}-\omega_{\mathbf{k}+\mathbf{q}_1}-\mathrm{i}\eta)} \\ & + \frac{n_{\mathbf{k}+\mathbf{q}_1}(1-n_{\mathbf{k}})(1-n_{\mathbf{k}+\mathbf{q}})}{(-q_1^0+\omega_{\mathbf{k}+\mathbf{q}_1}-\omega_{\mathbf{k}}-\mathrm{i}\eta)(q^0-q_1^0+\omega_{\mathbf{k}+\mathbf{q}_1}-\omega_{\mathbf{k}+\mathbf{q}}+\mathrm{i}\eta)} \\ & - \frac{(1-n_{\mathbf{k}+\mathbf{q}_1})n_{\mathbf{k}}n_{\mathbf{k}+\mathbf{q}}}{(-q_1^0+\omega_{\mathbf{k}+\mathbf{q}_1}-\omega_{\mathbf{k}}-\mathrm{i}\eta)(q^0-q_1^0+\omega_{\mathbf{k}+\mathbf{q}_1}-\omega_{\mathbf{k}+\mathbf{q}}+\mathrm{i}\eta)} \\ & + (q_1 \to q-q_1)], \end{aligned} \tag{2.15}$$

where $n_{\mathbf{q}} = \Theta(q_F - |\mathbf{q}|)$, $\omega_{\mathbf{k}} = \mathbf{k}^2/2$, and η is a positive infinitesimal.

Analytical evaluation of Eq. (2.12) results in the non-interacting linear density-response function of Stern[10]. As for the non-interacting quadratic density-response function, we first sum occupation numbers in Eq. (2.15) to find

$$\begin{aligned} Y_{q,-q_1}^0 = -\int \frac{\mathrm{d}^2\mathbf{k}}{(2\pi)^2} n_{\mathbf{k}}[\quad & \frac{1}{q^0+\omega_{\mathbf{k}}-\omega_{\mathbf{k}+\mathbf{q}}+\mathrm{i}\eta}\,\frac{1}{q_1^0+\omega_{\mathbf{k}}-\omega_{\mathbf{k}+\mathbf{q}_1}+\mathrm{i}\eta} \\ & + \frac{1}{-q^0+\omega_{\mathbf{k}}-\omega_{\mathbf{k}+\mathbf{q}}-\mathrm{i}\eta}\,\frac{1}{-(q^0-q_1^0)+\omega_{\mathbf{k}}-\omega_{\mathbf{k}+\mathbf{q}-\mathbf{q}_1}-\mathrm{i}\eta} \\ & + \frac{1}{-q_1^0+\omega_{\mathbf{k}}-\omega_{\mathbf{k}+\mathbf{q}_1}-\mathrm{i}\eta}\,\frac{1}{(q^0-q_1^0)+\omega_{\mathbf{k}}-\omega_{\mathbf{k}-(\mathbf{q}-\mathbf{q}_1)}+\mathrm{i}\eta} \\ & + (q_1 \to q-q_1)]. \end{aligned} \tag{2.16}$$

For the real part, we find[21]:

$$\mathrm{Re}\left[Y_{q,-q_1}^0\right] = -\left[(I_{q,q_1}+I'_{q,q_1})+(I_{-q,-q+q_1}+I'_{-q,-q+q_1})+(I_{-q_1,q-q_1}-I'_{-q_1,q-q_1})\right], \tag{2.17}$$

where

$$I_{q,q_1} = \frac{1}{2\pi|\mathbf{q}||\mathbf{q}_1|\sin\chi}\{\arctan\left[\frac{A\sin\chi}{A_1 - A\cos\chi}\right] - \mathrm{sgn}A\arctan\left[\frac{\sin\chi\sqrt{A^2-q_F^2}}{A_1 - A\cos\chi}\right]\Theta(A^2-q_F^2)$$
$$+ \arctan\left[\frac{A_1\sin\chi}{A - A_1\cos\chi}\right] - \mathrm{sgn}A_1\arctan\left[\frac{\sin\chi\sqrt{A_1^2-q_F^2}}{A - A_1\cos\chi}\right]\Theta(A^2-q_F^2)\} \tag{2.18}$$

and

$$I'_{q,q_1} = -\Theta(q_F^2\sin^2\chi - G)\frac{1}{4|\mathbf{q}||\mathbf{q}_1|\sin\chi}. \tag{2.19}$$

Here $A = q^0/|\mathbf{q}| - |\mathbf{q}|/2$, $A_1 = q_1^0/|\mathbf{q}_1| - |\mathbf{q}_1|/2$, and $G = \sqrt{A^2 - 2AA_1\cos\chi + A_1^2}$, χ being the angle between $\mathbf{q}$ and $\mathbf{q}_1$.

As for the imaginary part of $Y^0_{q,-q_1}$ we define[5,6] the function H_{q,q_1}, which can be represented in terms of a sum over hole and particle states and gives the second order contribution to the so-called absorption probability, as demonstrated in Ref. 6. We find,

$$\mathrm{Im}\left[Y^0_{q,-q_1}\right] = H_{q,q_1} + H_{q_1,q} + H_{q-q_1,-q_1}, \tag{2.20}$$

where[21]

$$H_{q,q_1} = \frac{1}{2}\left[f_{q,q_1} - f_{-q,-q+q_1} + (q_1 \to q - q_1)\right] \tag{2.21}$$

and

$$f_{q,q_1} = \Theta(q_F^2 - A^2)\frac{1}{2\pi|\mathbf{q}||\mathbf{q}_1|\sin\chi}\ln\left|\frac{A_1 - A\cos\chi + \sin\chi\sqrt{q_F^2-A^2}}{A_1 - A\cos\chi - \sin\chi\sqrt{q_F^2-A^2}}\right|. \tag{2.22}$$

In particular, at low frequencies an expansion of H_{q,q_1} in powers of the frequency q^0 gives, after retaining only the first-order terms,

$$H^L_{q,q_1} = \Theta(4q_F^2 - |\mathbf{q}|^2)\frac{4(|\mathbf{q}|\cos\chi - |\mathbf{q}_1|)}{\pi|\mathbf{q}||\mathbf{q}_1|\left[|\mathbf{q}-\mathbf{q}_1|^2 - 4q_F^2\sin^2\chi\right]\sqrt{4q_F^2-|\mathbf{q}|^2}}\,q^0. \tag{2.23}$$

In the static limit ($q^0 \to 0$) both first and second order contributions to the absorption probability, $\mathrm{Im}\chi_q$ and H_{q,q_1}, are proportional to the frequency q^0, as in the case of a 3DEG.

III. ELECTRONIC STOPPING POWER

We consider an ion of charge Z_1 moving with constant velocity $\mathbf{v}$ at a fixed distance h from a 2DEG of density n_0. The Coulomb potential of this moving particle has the form

$$V(\mathbf{r}, z; t) = Z_1 |\mathbf{r} - \mathbf{v}t + (z - h)\hat{\mathbf{k}}|^{-1}, \tag{3.1}$$

where $\mathbf{r}$ represents, as in Eqs. (2.9) and (2.10), a two-dimensional position-vector in the 2D plane, and z denotes the coordinate normal to the 2DEG which we consider to be located at $z = 0$. Hence, in order to obtain the induced potential, we introduce this time-varying external potential into Eq. (2.1), and Eq. (2.1) into Eq. (2.5). We note that density-response functions of a 2DEG have their z arguments localized to the 2D plane by positional δ functions, we Fourier transform, and find, up to second order in Z_1:

$$\begin{aligned} V^{ind}(\mathbf{r}, z; t) = {} & Z_1 \int \frac{\mathrm{d}^2\mathbf{q}}{(2\pi)^2} \mathrm{e}^{\mathrm{i}(\mathbf{q}\cdot\mathbf{r} - \omega t) - |\mathbf{q}|(|z| + h)} v_{\mathbf{q}} \chi_{\mathbf{q},\omega} v_{\mathbf{q}} \\ & + Z_1^2 \int \frac{\mathrm{d}^2\mathbf{q}}{(2\pi)^2} \int \frac{\mathrm{d}^2\mathbf{q}_1}{(2\pi)^2} \mathrm{e}^{\mathrm{i}(\mathbf{q}\cdot\mathbf{r} - \omega t) - [|\mathbf{q}||z| + (|\mathbf{q}_1| + |\mathbf{q} - \mathbf{q}_1|)h]} v_{\mathbf{q}} Y_{\mathbf{q},\omega;-\mathbf{q}_1,-\omega_1} v_{\mathbf{q}_1} v_{\mathbf{q}-\mathbf{q}_1}, \end{aligned} \tag{3.2}$$

where $\omega = \mathbf{q} \cdot \mathbf{v}$ and $\omega_1 = \mathbf{q}_1 \cdot \mathbf{v}$.

The stopping power of the 2DEG is simply the retarding force that the polarization charge distribution in the vicinity of the projectile exerts on the projectile itself[22], and is given by

$$S = \frac{Z_1}{v} \int \mathrm{d}^2\mathbf{r} \int \mathrm{d}z \delta(\mathbf{r} - \mathbf{v}t) \delta(z - h) \nabla V^{ind}(\mathbf{r}, z; t) \cdot \mathbf{v}. \tag{3.3}$$

Substituting Eq. (3.2) into Eq. (3.3), we have[23]

$$\begin{aligned} S = {} & -\frac{Z_1^2}{v} \int \frac{\mathrm{d}^2\mathbf{q}}{(2\pi)^2} \omega \mathrm{e}^{-2|\mathbf{q}|h} v_{\mathbf{q}} \mathrm{Im}\left[\chi_{\mathbf{q},\omega}\right] v_{\mathbf{q}} \\ & - \frac{Z_1^3}{v} \int \frac{\mathrm{d}^2\mathbf{q}}{(2\pi)^2} \omega \int \frac{\mathrm{d}^2\mathbf{q}_1}{(2\pi)^2} \mathrm{e}^{-(|\mathbf{q}| + |\mathbf{q}_1| + |\mathbf{q} - \mathbf{q}_1|)h} v_{\mathbf{q}} \mathrm{Im}\left[Y_{\mathbf{q},\omega;-\mathbf{q}_1,-\omega_1}\right] v_{\mathbf{q}_1} v_{\mathbf{q}-\mathbf{q}_1}. \end{aligned} \tag{3.4}$$

In the RPA, χ_q and $Y_{q,-q_1}$ are obtained from Eqs. (2.11) and (2.12) or, equivalently, from

$$v_q \chi_q = K_q - 1 \tag{3.5}$$

and

$$Y_{q,-q_1} = K_q Y^0_{q,-q_1} K_{q_1} K_{q-q_1}, \tag{3.6}$$

where

$$K_q = \left(1 - \chi^0_q v_q\right)^{-1}. \tag{3.7}$$

The linear contribution to the stopping power of Eq. (3.4), which is proportional to Z_1^2, was evaluated in the RPA by Horing *et al*[13] at $T = 0$, and similar calculations were presented by Bret and Deutsch[14] at finite temperature. On the other hand, the quadratic contribution to the stopping power of Eq. (3.4) is, in the RPA and for a geometry with the ion-beam in-plane within the 2D electron layer ($h = 0$), equivalent to the result derived in Ref. 6, within many-body perturbation theory, as the energy loss per unit path length of the projectile, the integration space being now in two dimensions instead of three dimensions. This contribution to the stopping power, which is proportional to Z_1^3, discriminates between the energy loss of a proton and that of an antiproton, and appears as a consequence of losses to one- and two-step electronic excitations generated by both linearly and quadratically screened ion potentials, as discussed in Ref. 6.

In the case of slow intruders ($v \to 0$), only the low-frequency form of the response enters in the evaluation of Eq. (3.4). At zero frequencies both linear and quadratic density-response functions are real, $\mathrm{Im}\left[\chi^0_q\right]$ and H_{q,q_1} being at low frequencies proportional to the frequency q^0. Thus, retaining only the first-order terms in the frequencies, both Z_1^2 and Z_1^3 contributions to the stopping power are found to be proportional to the velocity of the projectile, as in a 3DEG. For the RPA quadratic contribution to the stopping power we find, after insertion of Eq. (2.23) into Eq. (3.4), the following result:

$$\left[S^L\right]^{(3)} = 8vZ_1^3 \int_0^\infty \frac{\mathrm{d}|\mathbf{q}|}{\sqrt{4q_F^2 - |\mathbf{q}|^2}} \int_0^\infty \mathrm{d}|\mathbf{q}_1| \int_0^\pi \mathrm{d}\chi \mathrm{e}^{-(|\mathbf{q}|+|\mathbf{q}_1|+|\mathbf{q}-\mathbf{q}_1|)h} \frac{f_1^L + f_2^L}{|\mathbf{q} - \mathbf{q}_1|}, \tag{3.8}$$

where

$$f_1^L = \Theta(2q_F - |\mathbf{q}|) K^2_{\mathbf{q},0} K_{\mathbf{q}_1,0} K_{\mathbf{q}-\mathbf{q}_1,0} Y^0_{\mathbf{q},0;\mathbf{q}_1,0} \tag{3.9}$$

and

$$f_2^L = -\Theta(2q_F - |\mathbf{q}|)\frac{|\mathbf{q}|\left(|\mathbf{q}|\cos\chi - |\mathbf{q}_1|\right)}{\pi|\mathbf{q}_1|\left(|\mathbf{q}-\mathbf{q}_1|^2 - 4q_F^2\sin^2\chi\right)}K_{\mathbf{q},0}K_{\mathbf{q}_1,0}K_{\mathbf{q}-\mathbf{q}_1,0}. \tag{3.10}$$

IV. RESULTS

In the low-velocity limit ($v \to 0$), the stopping power can be evaluated to all orders in Z_1, on the basis of a free-electron picture, with the additional assumption of independent, individual, elastic electron scattering, and it is easily found to be, in both two and three dimensions, proportional to the velocity of the projectile[24]. By using density-functional theory (DFT)[25] to calculate the self-consistent potential generated by a static charge submerged in a 3DEG, Echenique *et al*[26] evaluated the nonlinear stopping power of a 3DEG for slow ions. Nonlinear calculations for an in-plane projectile in 2D have been performed recently by using a nonlinearly screened scattering potential based on the Sjölander-Stott theory[17], with the use of a nonlinear version of the linearized Fermi-Thomas potential[18] in which the screening constant is determined from the Friedel sum rule, and on the basis of a self-consistent potential[27] obtained within DFT as in Ref. 26 for the 3D case.

The nonlinear calculations presented in Ref. 18 for the energy-loss of slow protons and antiprotons are very close to the calculations of Ref. 27 when exchange and correlation (XC) contributions to the DFT scattering potential are excluded. These calculations are correct to all orders in Z_1, and they represent, therefore, a good check for our quadratic response calculations, which should be exact in the high-density and/or low Z_1 limits. Nevertheless, the approaches of Refs. 17,18 and 27 have the limitation of being restricted to very low ion velocities ($v << v_F$, v_F being the Fermi velocity), while our nonlinear Z_1^3 corrections are valid for arbitrary non-relativistic velocities.

The low-velocity limit of the quadratic stopping power, as obtained from Eq. (3.8) for an in-plane ($h = 0$) moving charge and divided by the velocity, is represented in Fig. 2 by a solid line, as a function of the electron-density parameter r_s. Stars and squares

represent the full nonlinear contribution to the stopping power for antiprotons reported in Refs. 18 and 27, respectively, multiplied by a factor of -1, showing an excellent agreement, in the high-density limit, with our Z_1^3 nonlinear contribution. For $r_s \geq 2$, higher order corrections become important, and for $r_s > 3$, Z_1^2 contributions (dashed line) are smaller than the Z_1^3 correction, indicating that the external potential cannot be treated, for these electron densities, as a small perturbation. In the case of a projectile moving at a given h distance above the 2D plasma the external perturbation is obviously diminished and, in particular, for $h = 1/q_F$ the quadratic stopping power is smaller than the linear one for all electron densities (see the inset of Fig. 2). The full nonlinear contribution to the stopping power for protons reported in Refs. 18 and 27 for $h = 0$ is also represented in Fig. 2 by circles and crosses, respectively, showing large differences with our Z_1^3 calculations for all electron densities. These differences appear as a consequence of perturbation theory failing to describe electronic states bound to the proton, which in 2D systems can be supported by arbitrarily weak attractive potentials[28].

As the velocity of the projectile (v) and/or the distance from the 2D plasma (h) increase, the ion potential becomes a relatively smaller perturbation and the Z_1^3 contribution to the stopping power for antiprotons may, therefore, be expected to approximately describe the full nonlinear contribution to the stopping power for arbitrary values of v and h, as long as $r_s < 2$, and also for lower densities ($r_s \geq 2$) as the velocity and the h distance increase. Substitution of the full RPA linear and quadratic 2DEG density-response functions of Eqs. (3.5) and (3.6) into Eq. (3.4) results in the quadratic stopping power plotted by a solid line in Fig. 3, as a function of the impinging projectile velocity, for $r_s = 1$ and $h = 0$, and also for $r_s = 1$ and $h = 1/q_F$ (see the inset of Fig. 3). The dotted line represents the low-velocity limit, as obtained from Eq. (3.8), and dashed lines represent linear RPA contributions to the stopping power of Eq. (3.4).

The quadratic contribution to the stopping power of a 2DEG presents properties not shared by the 3DEG. First, the range of validity of the linear velocity dependence of this contribution to the stopping power (see Fig. 3) persists only up to velocities much smaller

than the Fermi velocity, in contrast to the 3D situation in which the linear velocity dependence persists up to velocities approaching the Fermi velocity[6]. Second, at velocities around the plasmon threshold velocity, for which the projectile has enough energy to excite a plasmon[29], the ratio between Z_1^3 and Z_1^2 contributions to the stopping power increases, again in contrast to the 3D situation. Furthermore, we have found that the increase of this ratio at the plasmon threshold velocity becomes dramatic as the electron density decreases. Of course, the ratio between quadratic and linear contributions to the stopping power decreases very rapidly with h (see the inset of Fig. 3), but the relative, and for large r_s dramatic, increase of this ratio at the plasmon threshold velocity persists for all values of h that are not much larger than $1/q_F$. For a 2DEG the group velocity of the plasmon wave nearly coincides with the plasmon threshold velocity of the projectile (see Fig. 4); also, the inclusion of short-range correlations, which are ignored in the RPA, is known to have a substantial effect on the plasmon dispersion[30]. We interpret the anomalous enhancement of the ratio between quadratic and linear contributions to the stopping power at the plasmon threshold velocity and small electron densities ($r_s > 1$) as a result of neglecting, within the RPA, short-range correlations between the electrons of a 2D system, since these correlations are non-negligible for all values of h as long as r_s is not small.

V. CONCLUSIONS

We have presented an analytical evaluation of the wave-vector and frequency dependent non-interacting quadratic density-response function of a 2DEG. We have used this result to find, within a self-consistent field approximation, the Z_1^3 correction to the stopping power of a 2DEG for charged recoiless particles moving at a fixed distance from the 2D plasma sheet. We have reproduced, in the high-density limit, previous full nonlinear calculations of the stopping power of a 2DEG for slow antiprotons, and we have gone further to calculate the Z_1^3 correction to the stopping power for a wide range of projectile velocities. We have found that the Z_1^3 contribution to the stopping power of a 2DEG presents properties not shared

by the 3DEG. On the one hand, the range of validity of the linear velocity dependence of the Z_1^3 contribution to the stopping power persists only up to velocities much smaller than the Fermi velocity, and, on the other hand, an anomalous enhancement of the ratio between quadratic and linear contributions to the stopping power at the plasmon threshold velocity is found, within the RPA, at small electron densities ($r_s > 1$). Also, our results indicate that linear response calculations are, for all projectile velocities, less reliable in 2D than in 3D.

ACKNOWLEDGMENTS

We acknowledge partial support by the University of the Basque Country, the Basque Unibertsitate eta Ikerketa Saila, the Spanish Ministerio de Educación y Cultura, and Iberdrola SA.

REFERENCES

[1] D. Bohm and D. Pines, Phys. Rev. **92**, 609 (1953).

[2] J. Lindhard, K. Dan. Vidensk. Selsk. Mat.- Fys. Medd. **28** (8), 1 (1954).

[3] R. Cenni and P. Saracco, Nucl. Phys. A **487**, 279 (1988).

[4] C. F. Richardson and N. W. Ashcroft, Phys. Rev. B **50**, 8170 (1994); J. M. Rommel and G. Kalman, Phys. Rev. B **54**, 3518 (1996).

[5] J. M. Pitarke, R. H. Ritchie, P. M. Echenique, and E. Zaremba, Europhys. Lett. **24**, 613 (1993); J. M. Pitarke, R. H. Ritchie, and P. M. Echenique, Nucl. Instrum. Methods B **24**, 613 (1993).

[6] J. M. Pitarke, R. H. Ritchie, and P. M. Echenique, Phys. Rev. B **52**, 13882 (1995).

[7] T. Ando, A. Fowler, and F. Stern, Rev. Mod. Phys. **54**, 437 (1982).

[8] J. R. Engelbrecht and M. Randeira, Phys. Rev. Lett. **65**, 1032 (1990); P. W. Anderson, Phys. Rev. Lett. **64**, 1839 (1990).

[9] R. H. Ritchie, Phys. Rev. **106**, 874 (1957); R. H. Ritchie, Surf. Sci. **34**, 1 (1973).

[10] F. Stern, Phys. Rev. Lett. **18**, 546 (1967).

[11] A. K. Rajagopal and J. C. Kimball, Phys. Rev. B **15**, 2819 (1977).

[12] A. V. Chaplik, Zh. Eksp. Teor. Fiz. **60**, 1845 (1971); G.F. Giuliani and J.J. Quinn, Phys. Rev. **B26**, 4421 (1982); L. Zheng and S. D. Sarma, Phys. Rev. B **53**, 9964 (1996).

[13] N. J. M. Horing, H. C. Tso, and G. Gumbs, Phys. Rev. **B36**, 1588 (1987).

[14] A. Bret and C. Deutsch, Phys. Rev. **E48**, 2994 (1993).

[15] Y.-N. Wang and T.-C. Ma, Phys. Lett. A **200**, 319 (1995).

[16] A. Bergara, I. Nagy, and P. M. Echenique, Phys. Rev. B **55**, 12864 (1997).

[17] A. Krakovsky and J.K. Percus, Phys. Rev. B **52**, R2305 (1995).

[18] Y.-N. Wang and T.-C. Ma, Phys. Rev. A **55**, 2087 (1997).

[19] C. D. Hu and E. Zaremba, Phys. Rev. B **37**, 9268 (1988); A. Bergara, I. Campillo, J. M. Pitarke, and P. M. Echenique, Phys. Rev. B **56**, 15654 (1997).

[20] Differences between the retarded density-response functions of Eqs. (2.14) and (2.15), on the one hand, and time-ordered response functions, as defined within many-body theory (see, e.g., G. D. Mahan, *Many-Particle Physics* (Plenum, New York, 1981)), on the other hand, lie in $\omega + \mathrm{i}\eta$, which should be replaced in Eqs. (2.14) and (2.15) by $\omega + \mathrm{i}\eta\mathrm{sgn}(\omega)$ [ω being either q^0, q_1^0 or $(q^0 - q_1^0)$] in order to obtain their time-ordered counterparts.

[21] I'_{q,q_1}, $I'_{-q,-q+q_1}$ and $I'_{-q_1,q-q_1}$ in Eq. (2.17) should be multiplied by $\mathrm{sgn}(q^0)\mathrm{sgn}(q_1^0)$, $\mathrm{sgn}(q^0)\mathrm{sgn}(q^0 - q_1^0)$ and $\mathrm{sgn}(q_1^0)\mathrm{sgn}(q^0 - q_1^0)$, respectively, to obtain the real part of the corresponding time-ordered quadratic response function. Similarly, the right-hand side of Eq. (2.21) should be multiplied by $\mathrm{sgn}(q^0)$ in order to obtain the imaginary part of the time-ordered quadratic response function.

[22] P. M. Echenique, F. Flores, and R. H. Ritchie, Solid State Phys. **43**, 229 (1990).

[23] The real parts of χ_q and $Y_{q,-q_1}$ give no contribution to the integrals of Eq. (3.4), since $\mathrm{Re}\,[\chi_q] = \mathrm{Re}\,[\chi_{-q}]$ and $\mathrm{Re}\,[Y_{q,q_1}] = \mathrm{Re}\,[Y_{-q,-q_1}]$.

[24] I. Nagy, Phys. Rev. **B51**, 77 (1995).

[25] P. Hohenberg and W. Kohn, Phys. Rev. **136**, B864 (1964); W. Kohn and L. J. Sham, *ibid.* **140**, A1133 (1965).

[26] P. M. Echenique, R. M. Nieminen, and R. H. Ritchie, Solid State Commun. **37**, 779 (1981); P. M. Echenique, R. M. Nieminen, J. C. Ashley, and R. H. Ritchie, Phys. Rev. A **33**, 897 (1986).

[27] E. Zaremba, P. M. Echenique, and I. Nagy, to be published.

[28] E. N. Economou, *Green's Functions in Quantum Physics* (Springer-Verlag, Berlin, 1990), pg. 64.

[29] At long wavelengths the plasma frequency in the 2DEG varies like $q^{1/2}$, in contrast to the 3D case (see, e. g., A. L. Fetter, Ann. Phys. (N.Y.) **81**, 367 (1973)). At short wavelengths, the group velocity of the 2D plasmon is nearly constant and approaches the plasmon threshold velocity, $v_{\rm th}$. For $r_s = 1$, $v_{\rm th} = 2.02 v_0$ (v_0 is Bohr's velocity).

[30] A. Gold and L. Calmels, Phys. Rev. **B48**, 11622 (1993).

FIGURES

FIG. 1. Diagrammatic interpretation of the RPA integral equations (2.6) and (2.7) for (a) linear and (b) quadratic density-response functions, respectively. Electron-hole empty and full bubbles represent non-interacting and interacting linear density-response functions, respectively. Empty and full triangles represent non-interacting and interacting quadratic density-response functions, respectively. The interacting RPA quadratic density-response function is obtained by summing over the infinite set of diagrams that combine three strings of empty bubbles (two-electron loops) through an empty three-electron loop. Dashed lines represent the electron-electron bare Coulomb interaction.

FIG. 2. Low-velocity limit of the Z_1^3 stopping power, as obtained from Eq. (3.8) (solid line) for $h = 0$ and $Z_1 = 1$, divided by the velocity, as a function of r_s; the corresponding Z_1^2 stopping power is represented by a dashed line. Full nonlinear contributions to the stopping power for antiprotons [$Z_1 = -1$] (stars and squares) and protons [$Z_1 = 1$] (circles ans crosses) have been obtained by subtracting RPA linear calculations from the results of Ref. 18 (stars and circles) and Ref. 27 [with XC contributions to the DFT scattering potential excluded] (squares and crosses), and dividing by Z_1; thus, the negative values at $r_s > 1$ simply mean that the full nonlinear stopping power lies, in the case of protons, below the linear results. The inset exhibits Z_1^2 and Z_1^3 contributions to the stopping power (dashed and solid lines, respectively) for $h = 1/q_F$ and $Z_1 = 1$.

FIG. 3. Full RPA Z_1^3 stopping power, as obtained from Eq. (3.4) (solid line) for $Z_1 = 1$, $h = 0$ and $r_s = 1$, as a function of the velocity of the projectile. The corresponding Z_1^2 stopping power is represented by a dashed line, and the dotted line represents the low-velocity limit of the Z_1^3 term. The inset shows the same results for $h = 1/q_F$.

FIG. 4. Two-dimensional RPA plasmon dispersion relation (solid line) and maximum energy transfer ($\omega_{max} = qv$) at the plasmon threshold velocity (dotted line), as functions of the wave number. The electron density parameter has been taken to be $r_s = 1$, thus the plasmon threshold velocity being $v_{th} = 2.02 v_0$ (v_0 is Bohr' velocity).

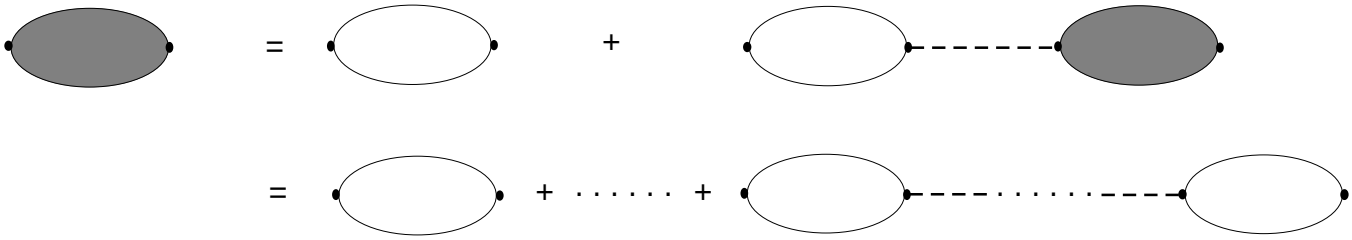

Figure 1a

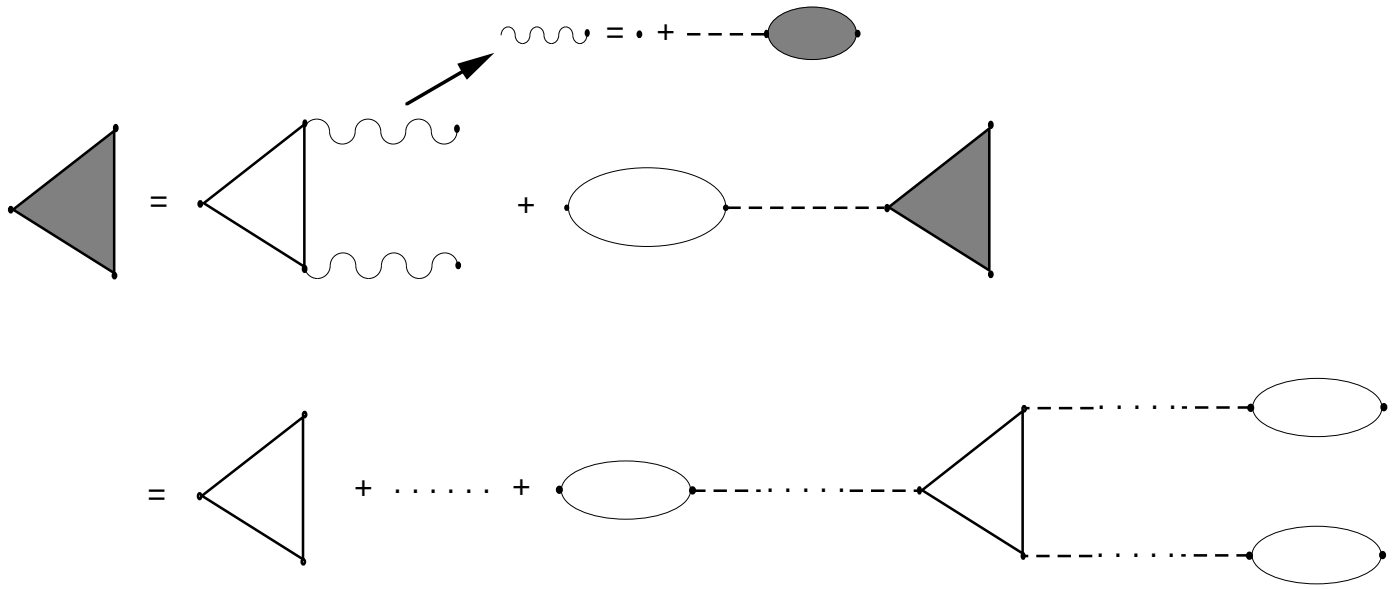

Figure 1b

Fig. 2

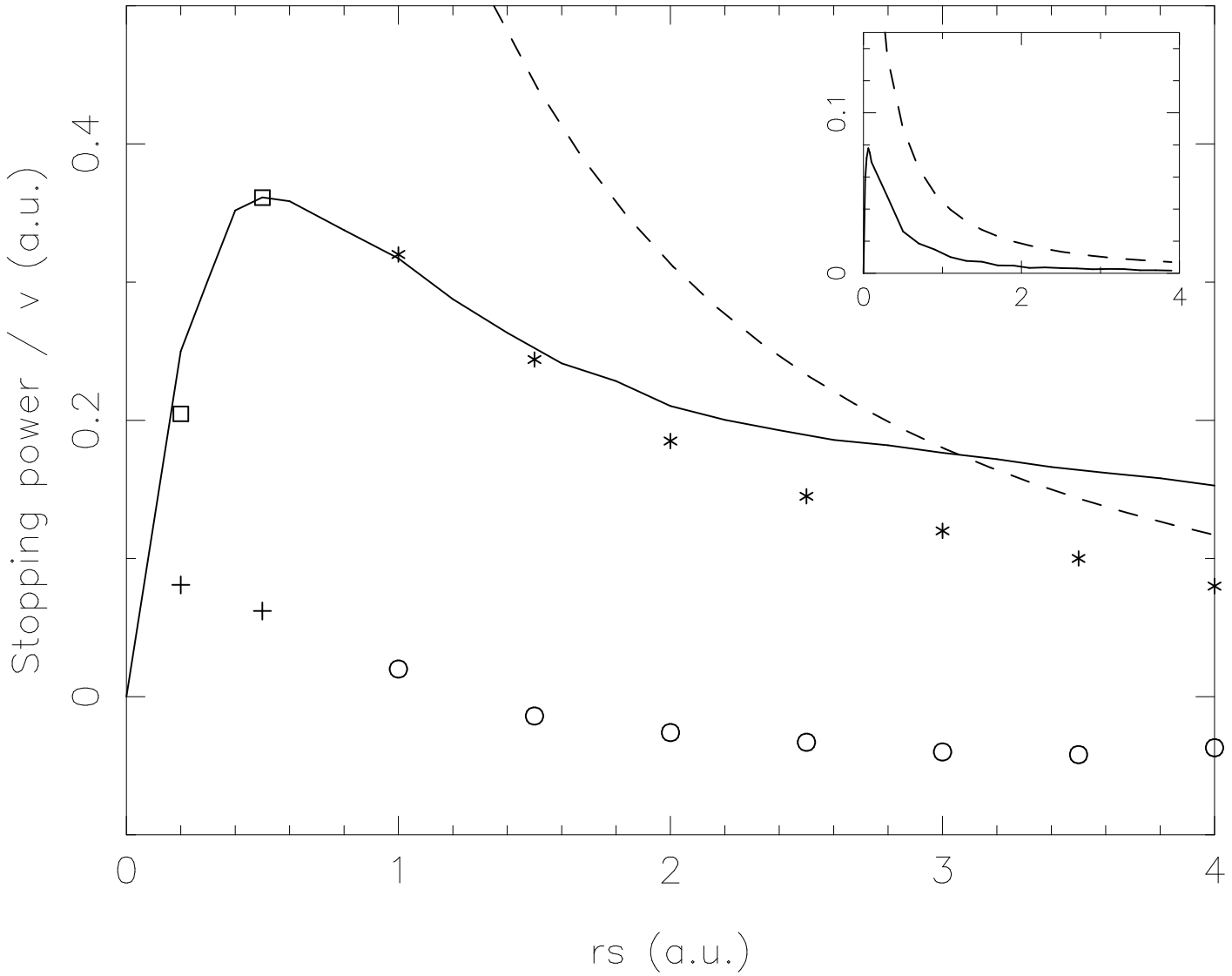

Fig. 3

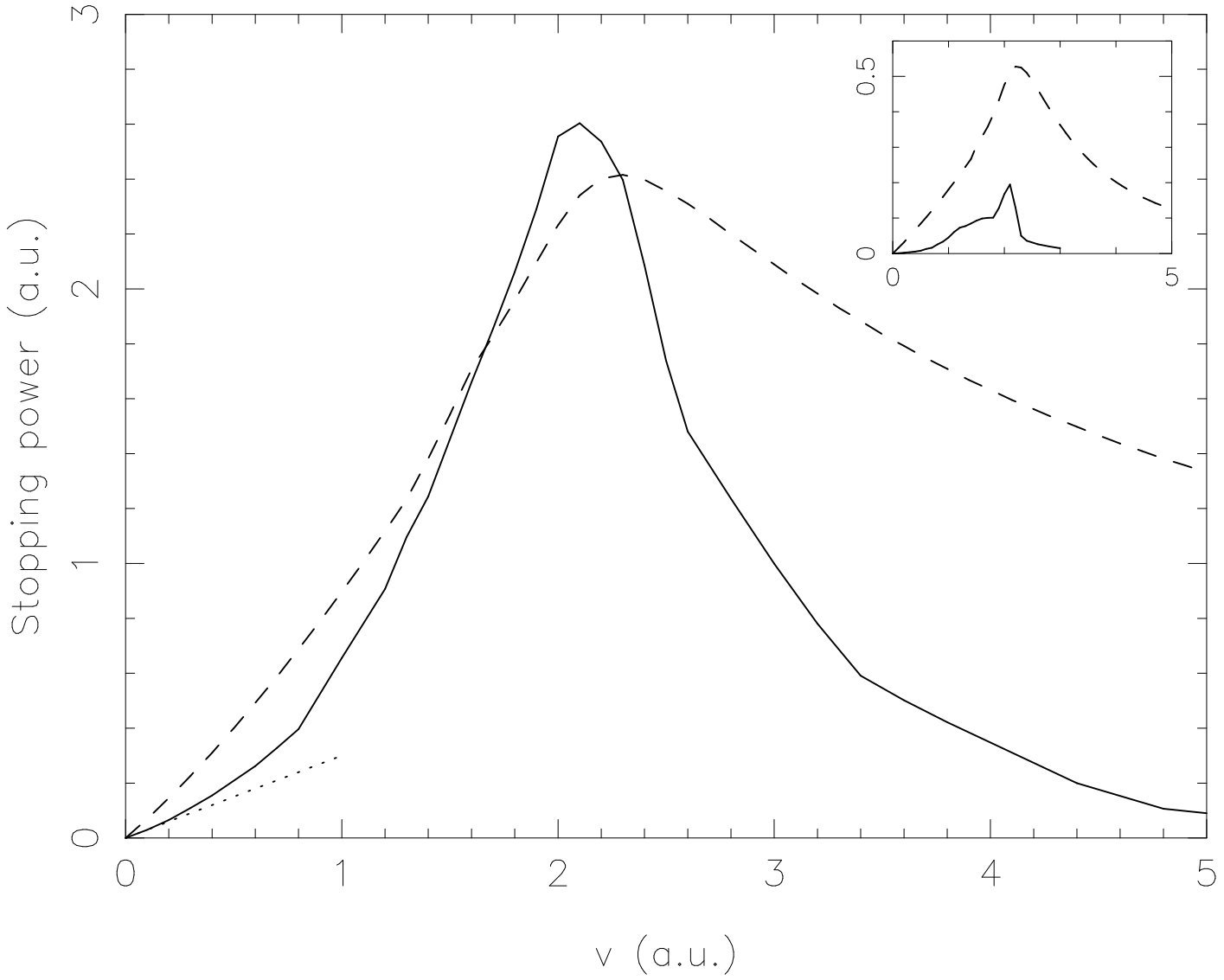

Fig. 4